

Launching and Controlling Gaussian Beams from Point Sources via Planar Transformation Media

Hayrettin Odabasi^{1,*}, Kamalesh Sainath², and Fernando L. Teixeira³

¹*Department of Electrical and Electronics Engineering,
Eskisehir Osmangazi University, Eskisehir, Turkey,*

²*Sandia National Laboratories, Albuquerque, New Mexico, USA, and*

³*ElectroScience Laboratory, The Ohio State University, Columbus Ohio, USA.*

(Dated: November 10, 2018)

Based on operations prescribed under the paradigm of Complex Transformation Optics (CTO) [1–4], it was recently shown in [5] that a complex source point (CSP) can be mimicked by a parity-time transformation media. Such coordinate transformation has a mirror symmetry and results in a balanced loss/gain metamaterial slab. A CSP produces a Gaussian beam and, consequently, a point source placed at the center of such metamaterial slab produces a Gaussian beam propagating away from the slab surface. Here, we extend the CTO analysis to non-symmetric complex coordinate transformations and show that, by using simply a (homogeneous) doubly anisotropic gain-media metamaterial slab, one can still mimic a CSP and produce Gaussian beam. Notably, we show that a Gaussian beam can be produced by point sources placed *outside* the slab as well. By making use of the extra degrees of freedom provided by CTO, the near-zero requirement on the real part of the resulting constitutive parameters can be relaxed to facilitate potential realization. In addition, exploitation of both real and imaginary parts of the CTO design yield direct control of the Gaussian beam properties such as peak amplitude and waist (focus) location.

PACS numbers:

I. INTRODUCTION

There has been an increased interest in complex transformation optics (CTO) [1–5] as a tool for designing metamaterials with functionalities beyond the reach of conventional TO [6–8]. Both TO and CTO rely on the known duality between metric and material properties in Maxwell’s equations [1, 2] to provide a pathway for designing metamaterial blueprints that mimic a change on the metric of space [9]. While TO is restricted to real-valued coordinate transformations, CTO employs complex-valued space transformations in a frequency-domain representation. Noteworthy examples of CTO-derived media are perfectly matched layers (PMLs), which are reflectionless absorbers extensively used to truncate the spatial domain in computational simulations [10–12]. Although their introduction was initially motivated strictly by simulation needs, PMLs also serve as blueprints for anisotropic absorbers [3, 12–16].

It is well known that a Gaussian beam can be recognized as the field produced by a complex source point (CSP) with imaginary displacement along the axial beam direction [17–21]. It was shown in [5] that a CSP can be realized using parity-time (\mathcal{PT}) metamaterials with a particular mirror-symmetric CTO transformation. This results on balanced gain/loss metamaterial slab that produces a unidirectional Gaussian beam.

In this work, we extend such ideas by showing that CSP, and consequently Gaussian beams, can be produced

more generally from point sources by transformation media comprised of doubly anisotropic gain-media metamaterial slabs that do not require \mathcal{PT} symmetry. Notably, by using CTO properties, we show that Gaussian beams can be produced even when the point source is located *outside* the slab. We further explore the use of a real stretching parameter in combination with the imaginary stretching parameter in the CTO transformation to control the (effective) CSP location and, as a result, Gaussian beam properties such as peak amplitude and waist (focus) location.

II. FORMULATION

Throughout the paper the $e^{-i\omega t}$ convention is assumed and omitted. Let us assume the following CTO mapping from real space (x, y, z) to complex space (x', y, z) :

$$x'(x) = \begin{cases} x'_0 + d/2 + x & \text{if } x \leq -d/2 \\ \int_{d/2}^x s_x(x) dx & \text{if } -d/2 \leq x \leq d/2 \\ x & \text{if } d/2 \leq x \end{cases} \quad (1)$$

where $x'_0 = x'(-d/2)$, $s_x(x) = a_x(x) + i\sigma_x(x)$ is a complex stretching factor, and d is the slab thickness. Using the (C)TO approach, the associated constitutive tensors [27] are obtained as $[\epsilon] = \epsilon_0[\Lambda]$ and $[\mu] = \mu_0[\Lambda]$, with $[\Lambda] = \det([S])^{-1} [S] [S]^T$, where $[S]$ is the Jacobian of the transformation in eq. (1) [1, 6, 8], i.e.

$$[\Lambda] = \begin{cases} \text{diag}(1, 1, 1) & \text{if } x \leq -d/2 \\ \text{diag}(s_x^{-1}, s_x, s_x) & \text{if } -d/2 \leq x \leq d/2 \\ \text{diag}(1, 1, 1) & \text{if } d/2 \leq x \end{cases} \quad (2)$$

*Corresponding author. Email: hodabasi@ogu.edu.tr

Note that the coordinate transformation needs to be continuous to avoid reflections or scattering. Clearly, this is satisfied by Eq.(1) as long as a_x and σ_x are bounded functions. The material tensor corresponds to a lossy or gain media if σ_x is chosen positive or negative, respectively [28]. The parameter a_x controls the real stretching and can be chosen so as to increase (if $a_x > 1$) or decrease ($a_x < 1$) the *electric* size of the slab. In particular, the electric size of the slab shrinks to zero in the limit $a_x \rightarrow 0$, which means that no phase accumulation occurs as the wave propagates through the slab. In addition, the choice $a_x < 0$ produces negative refraction effects [29].

Here we compare two alternative choices for the σ_x parameter:

(a) *Balanced loss/gain \mathcal{PT} media* [5]:

$$\sigma_x = \mp 2b/d \quad \text{for } x \gtrless 0, |x| \leq d/2, \quad (3)$$

with $b > 0$. Due to the mirror symmetry of this σ_x profile, the material tensors are \mathcal{PT} symmetric, i.e. $\epsilon(x) = \epsilon^*(-x)$ and the metamaterial slab corresponds to a balanced loss/gain media. The corresponding value of $\Im m[x']$ is shown in the red curve in Fig. 1.

(b) *Doubly anisotropic gain-media*:

$$\sigma_x = -b/d \quad \text{for } |x| \leq d/2, \quad (4)$$

again with $b > 0$. The corresponding behavior of $\Im m[x']$ is shown by the green curve in Fig. 1.

By choosing $a_x = 0$ in both cases, one obtains $\Re e[x']$ as shown by the blue curve in Fig. 1. Both cases provide the necessary imaginary component required for the realization of CSP. However, there is a major difference between them in that for $x < -d/2$ (i.e. outside the slab) $\Im m[x'] = 0$ in case (a) whereas $\Im m[x'] > 0$ in case (b). Note that this occurs even though $[\Lambda] = \text{diag}(1, 1, 1)$ (corresponding to free-space) in that region for both cases. At first sight, this result may seem paradoxical, but really what happens in this case is that the doubly anisotropic gain-medium metamaterial slab amplifies the fields from sources placed *outside* it, so that in the transformed problem the point source appears mapped to complex space. This enables such metamaterial slab to be used as a Gaussian beam launcher. Note that such coordinate transformation is bidirectional; in other words, the same effect is obtained whether we place the source at $x \leq -d/2$ or $x \geq d/2$. Here, we placed the source at $x \leq -d/2$.

III. RESULTS AND DISCUSSION

The field due to a line source of $\vec{J}' = \hat{z}\delta(x' - x'_s)\delta(y' - y'_s)$ is obtained analytically as [22]:

$$\vec{E}' = -\hat{z}\frac{I_0 k_0 \eta_0}{4} H_0^{(1)}(k_\rho R') \quad (5)$$

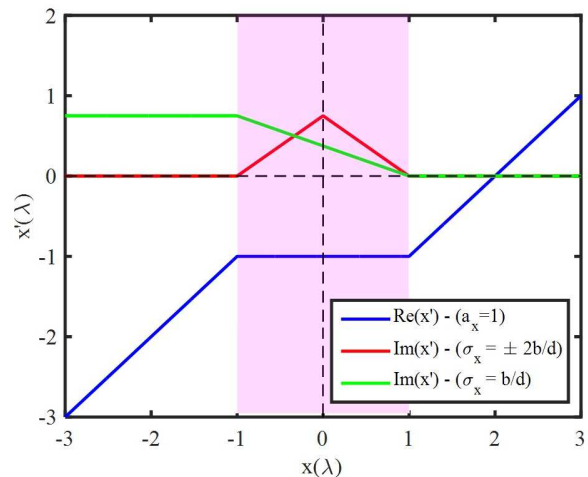


FIG. 1: Coordinate transformations showing the real and imaginary parts of the transformed coordinate x' as a function of the original coordinate x , as entailed by Eqs. (1), (3), and (4). Colored area indicates the metamaterial slab region, $|x| \leq d/2$ with $d = 2\lambda$. The red curve corresponds to $\Im m[x']$ with $\sigma_x = \mp 2b/d$ for $x \gtrless 0$. The green curve corresponds to $\Im m[x']$ with $\sigma_x = -b/d$. The blue curve shows $\Re e[x']$, from $a_x = 0$ for $|x| \leq d/2$. Note that with $\sigma_x = \mp 2b/d$, $\Im m[x']$ reverts to zero outside of the slab. On the other hand, with $\sigma_x = -b/d$ there is a remnant positive value for $\Im m[x']$ in the transformed space outside the slab.

where $H_0^{(1)}$ is the Hankel function of first kind and zeroth order. The solution in the transformed coordinates is found by substituting the complex distance R' given by

$$R' = \sqrt{(x' - x'_s)^2 + (y' - y'_s)^2} \quad (6)$$

where (x'_s, y'_s) is the CSP location associated to a point source at (x_s, y_s) after the transformation given by Eq. 1. In order to obtain the proper field solution, a branch cut with $\Re e[R'] > 0$ (the so-called source-type solution) is chosen [17–21]. The actual fields \vec{E} and sources \vec{J} in real space is found simply [1, 6, 8] by

$$\vec{E} = [S^{-1}]^T \cdot \vec{E}'. \quad (7a)$$

$$\vec{J} = \det([S])^{-1} [S] \cdot \vec{J}'. \quad (7b)$$

In what follows, we show analytical results for the CSPs produced by various CTO mappings together with simulation results based on the ComsolTM finite element (FE) software for point sources placed near or inside metamaterial slabs with constitutive tensors given by Eq. (2-4). We assume $b = 0.75\lambda$ and $d = 2\lambda$, where λ is the wavelength.

A. Results for $a_x = 0$

Fig. 2 (a,e) shows contour plots of $\Im m[R']$ and $\Re e[E_z]$ based on the analytical solution for a standard CSP at

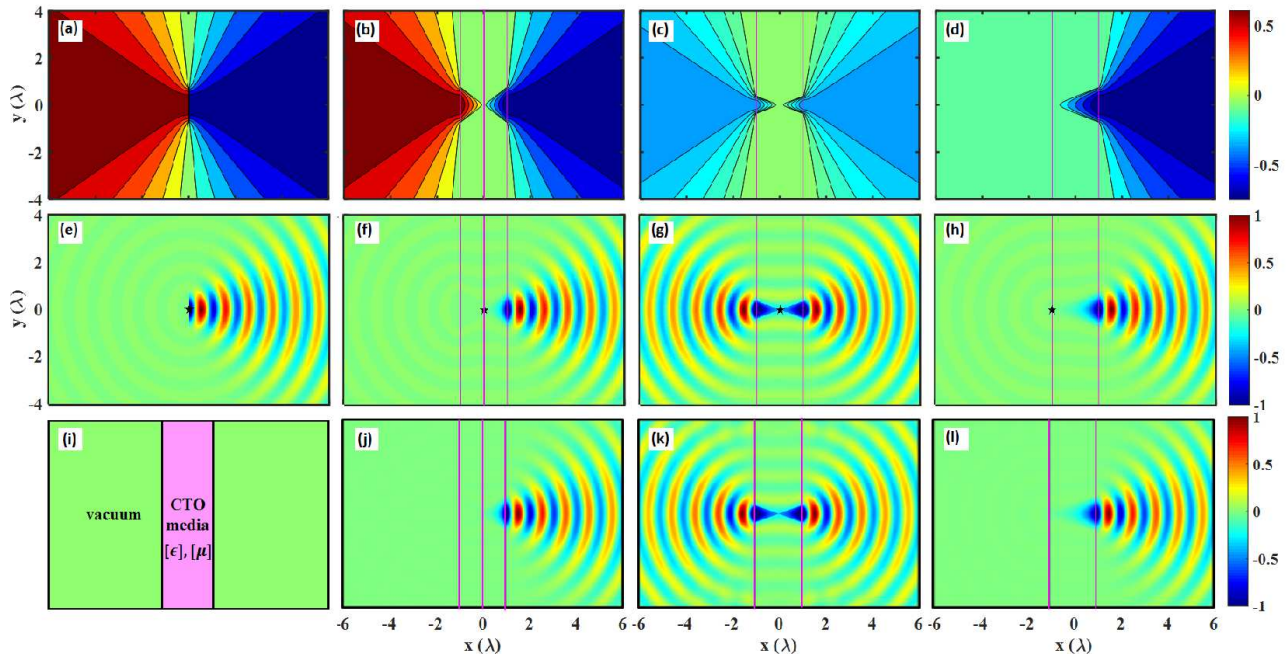


FIG. 2: Summary of CTO approach to obtain blueprints for planar metamaterial slabs that generate Gaussian beams from a point source placed in or next to it. (a): Contour plots of $\Im m[R']$ for a CSP placed at $(ib, 0)$ in free-space, with $b = 0.75\lambda$. (b): Contour plots of $\Im m[R']$ due to point source placed at the center of the PT -symmetric metamaterial slab. In this and all other cases considered here the slabs comprise the region $|x| \leq d/2$ with $d = \lambda$. (c, d): Contour plots of $\Im m[R']$ for a point source located at the center and at the left boundary, respectively, of a doubly anisotropic gain-medium metamaterial slab with $a_x = 0$ and $\sigma_x = -b/d$. (e-h): Field distributions of $\Re e[E_z]$ based on the analytical solution, Eqs. (5) and (6), corresponding to cases (a-d), respectively. The source points are indicated by the star symbols. (i) Geometry of the problem. The point source is placed inside or next to the metamaterial slab. (j-l): FE simulation results with metamaterial slabs corresponding to (b-d), respectively. In all field plots of this paper, $\Re e[E_z]$ is normalized to the $[-1, 1]$ interval.

$(x_s, y_s) = (i0.75, 0)\lambda$, where the Gaussian beam distribution is clearly visible. Fig. 2 (b,f) shows $\Im m[R']$ and $\Re e[E_z]$ for a point source placed at $(x_s, y_s) = (0, 0)$ followed by transformation set by Eq. (3) so that $(x'_s, y'_s) = (ib, 0)$, corresponding to the balanced loss/gain \mathcal{PT} case. The associated constitutive tensors have $[\Lambda] = \mp \text{diag}(id/2b, -i2b/b, -i2b/d)$ for $x \geq 0$ and $|x| \leq d/2$ [30]. Note that in this case, there is no Gaussian beam generation if the point source is placed at $|x| \geq d/2$ (i.e. outside the slab) since the corresponding CSP would revert to a real-valued point. This can also be understood by the fact, for a balanced loss-gain media, any field amplification over the gain section of the slab would then be compensated by field attenuation over the loss section. Fig. 2 (c,g) shows the contour plots of $\Im m[R']$ and $\Re e[E_z]$ for a point source placed at $(x_s, y_s) = 0$ followed by the transformation defined in Eq. (4) so that $(x'_s, y'_s) = (ib/2, 0)$. This corresponds to the doubly anisotropic gain-media case with material tensors set by $[\Lambda] = \text{diag}(id/b, -ib/b, -ib/d)$ for $|x| \leq d/2$. For this particular $\sigma_x = ib/d$ choice, the beamwidth of the Gaussian beam is different from the standard CSP (Fig. 2 (a,e)) and \mathcal{PT} (Fig. 2 (b,f)) cases due to the different imaginary displacement for (x'_s, y'_s) . Fig. 2(d,h) shows results for the same transformation but now with

the point source placed at the left boundary of the slab, $x = -d/2$. In the transformed problem, this is equivalent to an ordinary source for observation points on the same side of slab and to a CSP for observation points on the opposite side of the slab. Consequently, the Gaussian beam is launched towards the opposite of the slab as a consequence of the field amplification as the wave traverses the slab. The beamwidth for this case is equivalent to the original CSP and \mathcal{PT} metamaterial cases since the CSP is at $(x_s, y_s) = (ib, 0)$. Fig 2 (i) illustrates the basic setup for the FE simulations. Fig. 2 (j-l) shows the FE simulation results with metamaterial slabs with constitutive properties set by the respective $[\Lambda]$.

B. Results for $a_x > 0$

In all the above cases, we have assumed $a_x = 0$ which entails material tensors with purely imaginary elements. Next, we show how it is possible to further control the Gaussian beam characteristics by varying a_x . Fig. 3 shows Gaussian beams produced from point sources at various x_s next to doubly anisotropic gain-media slabs based on Eqs.(1), (2), and (4) with different a_x . In all cases, $d = \lambda$ and $\sigma_x = -2b/d$. Fig. 3 (a) shows the

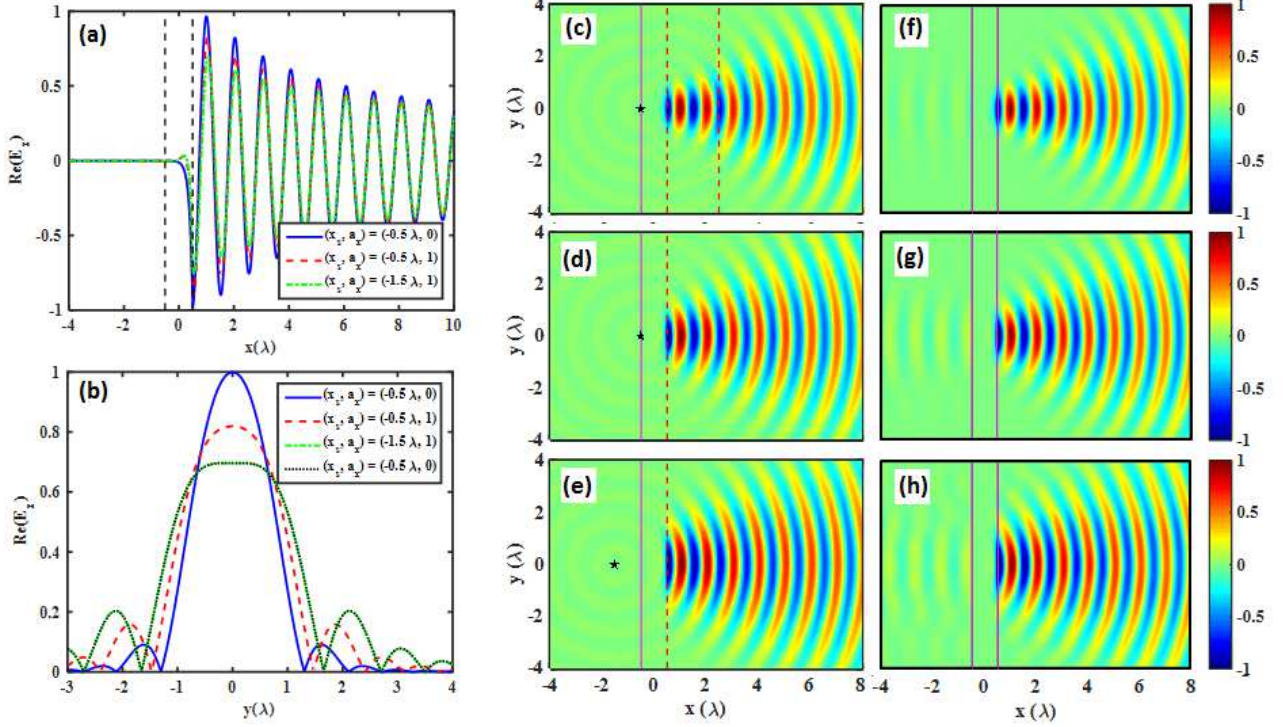


FIG. 3: Gaussian beam produced from point sources, as indicated by the star symbols, at different locations x_s next to doubly anisotropic gain-media slabs with different values for the real stretching parameter a_x . In all cases, $d = \lambda$ and $\sigma_x = -2b/d$. (a): $\Re[E_z]$ along the horizontal cut $y = 0$ for various choices of (x_s, a_x) , as indicated. (b): $\Re[E_z]$ along the vertical cuts $x = 0$ for the above three cases together with a vertical cut of $\Re[E_z]$ at $x = 2.5\lambda$ (red dashed lines) for $(x_s, a_x) = (-0.5\lambda, 0)$. (c-e): Analytical solutions based on Eq. (5)-(6) for the three cases of (x_s, a_x) considered in (a). The point source locations are indicated by the star symbols. Note that for $a_x = 0$, as shown in (c) and indicated by the blue curve in (a), there is no phase progression inside the slab, only amplification. In contrast, for $a_x = 1$ there is a phase progression inside the slab. As a consequence, the $\Re[E_z]$ distribution along the vertical cuts $x = 2.5\lambda$ in (c) and $x = 0$ in (e) are equal to each other, compare also the green and dashed lines in (b). (f-h): FE simulation results corresponding to (c-e).

$\Re[E_z]$ distribution along the horizontal cut $y = 0$ for different choices of x_s and a_x , namely: $(x_s, a_x) = (-\lambda, 0)$, $(-\lambda, 1)$, and $(-1.5\lambda, 1)$. Fig. 3 (b) shows $\Re[E_z]$ along the vertical cut $x = 0$, indicated by the red dashed line in Fig. 3 (c). In Fig. 3 (b) we also show $\Re[E_z]$ along the cut at $x = 2.5\lambda$ as indicated by the magenta dashed line in Fig. 3 (c). The plots in Fig. 3 (c-e) show the respective $\Re[E_z]$ distributions in space based on Eq. 4(5-7). Note that for $a_x = 0$, see Fig. 3 (c) and the blue trace in Fig. 3 (a), there is no phase progression inside the slab, only amplification. The effect of a_x is to change the electrical thickness and by setting $a_x > 0$, a phase progression is produced in the field within the slab, as visible in the $a_x = 1$ case. Note that the $\Re[E_z]$ distribution along $x = 2.5\lambda$ in Fig. 3 (c) and $x = 0$ in Fig. 3 (e) are equal to each other since they correspond to the same amount of amplification and phase progression. Compare also the green dash-dotted and black dotted lines in Fig. 3 (b).

C. Results for $a_x < 0$

Lastly, we consider the choice of negative a_x , which entail negative refraction effects [23, 24]. The case $a_x = -1$ and $\sigma_x = 0$ in particular recovers the isotropic Veselago slab [25] (other choices of a_x and σ_x lead to *anisotropic Veselago slabs* [26]) where foci can be established inside and outside the slab. Considering $\sigma_x = -b/d$ as in Eq. (4), this generalizes to a gain media in which beam waists are created inside and outside of the slab. Fig. 4 (a,d) shows $\Re[E_z]$ based on the analytical solution from Eqs. (5) and (6) for metamaterial slabs having $\sigma_x = -b/d$, and with $a_x = -1$ and $a_x = -2$ respectively. Fig. 4 (b,e) shows corresponding FE simulation results for a point source placed near the associated metamaterial slabs. As a reference, Fig. 4 (c,f) shows the associated analytical results considering $\sigma_x = 0$, wherein the two foci, one inside and the other outside the slab are clearly visible. From the plots, we observe that the locations of the Gaussian beam waists in the case $\sigma_x = -b/d$ coincide with the foci

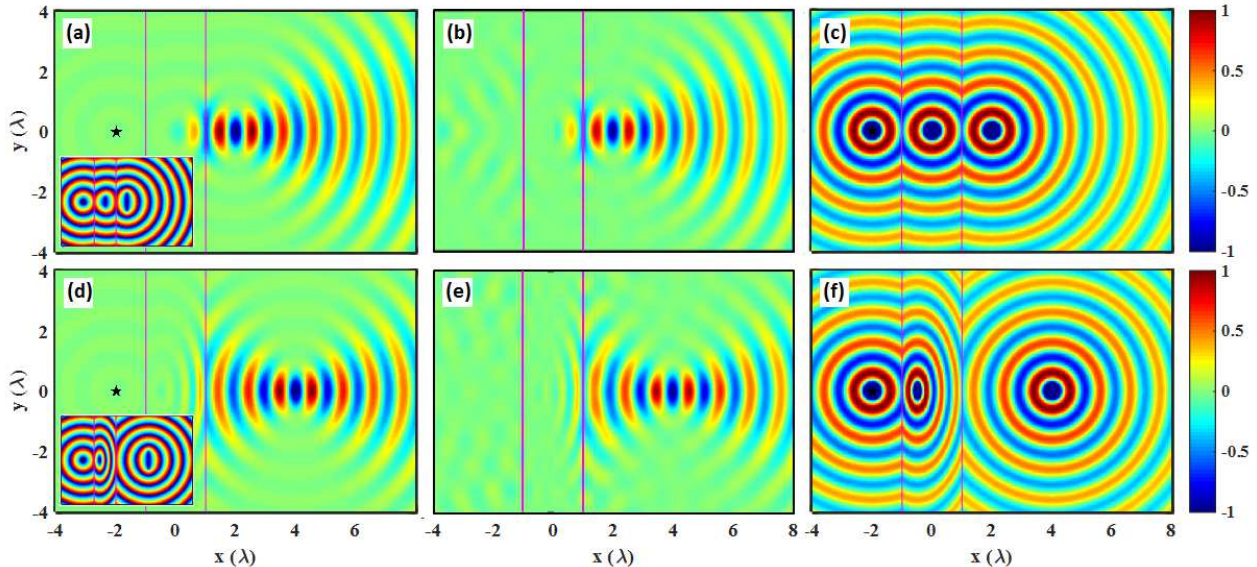


FIG. 4: Effect of negative a_x on the Gaussian beam generation. (a,d): $\Re[E_z]$ distributions based on the analytic solution, Eqs. (5) and (6), for a CSP mapped by $a_x = -1$ and $a_x = -2$ respectively, and with $\sigma_x = -b/d$ in Eq. (1). The insets show the phase distributions to highlight the foci. (b, e): Corresponding $\Re[E_z]$ field distributions based on FE simulations with doubly anisotropic gain-media metamaterial slabs. (c, g): Corresponding analytical solutions when $\sigma_x = 0$ (Veselago slab).

location in the $\sigma_x = 0$ case with same a_x . Moreover, it is seen that this location can be controlled by varying a_x . Note also that, although not visible in $\Re[E_z]$ plots due to the field amplification effects across the slab, in addition to the focus (waist) outside of the slab, there is also one present inside the slab, see the phase profiles insets in Fig. 4 (a,d). These phase profiles resemble the $\Re[R']$ of a CSP, which indirectly verifies the mapping of the real point source to a CSP at the focal point of the slab.

IV. CONCLUDING REMARKS

The contributions from this work are three-fold. First, it was shown that Gaussian beams can be generated from point sources placed inside or outside doubly anisotropic gain-media slabs without the need for \mathcal{PT} symmetry. Second, it was verified that the location of the equivalent complex point source (CSP), and hence beam properties, can be controlled by varying both the real and imaginary part of the CTO mapping equations. Third, by using negative values for the real part of the CTO

mapping equations, it was demonstrated that a real point source placed one side of the metamaterial slab can be mapped to an equivalent CSP on the opposite side of the metamaterial slab. The CSP location corresponds to the waist location of the Gaussian beam and can be moved away from the slab. These findings were verified by means of equivalent CSP analytical solutions and by FE simulations employing the derived doubly anisotropic gain-media slabs.

The study here was done in the Fourier domain assuming the linear regime. Because gain media are inherently nonlinear, this means that the present method of analysis is restricted to field amplitudes below the gain saturation threshold. The particular values for the gain-media parameters used here have been chosen for the sake of illustration. Although the resulting gain levels are unrealistic under present technology, more feasible gain levels may be obtained using thicker slabs, as noted in [5]. Nevertheless, the doubly anisotropic gain-media slabs proposed here can be chosen to be homogeneous and hence are inherently simpler than balanced loss/gain \mathcal{PT} slabs, which are necessarily inhomogeneous.

-
- [1] F. Teixeira and W. Chew, J. Electromagn. Waves Appl. **13**, 665 (1999).
 [2] F. L. Teixeira and W. C. Chew, Int. J. Num. Model. **13**,

- 441 (2000), ISSN 1099-1204.
 [3] H. Odabasi, F. L. Teixeira, and W. C. Chew, J. Opt. Soc. Am. B **28**, 1317 (2011).

- [4] B.-I. Popa and S. A. Cummer, *Phys. Rev. A* **84**, 063837 (2011).
- [5] G. Castaldi, S. Savoia, V. Galdi, A. Alù, and N. Engheta, *Phys. Rev. Lett.* **110**, 173901 (2013).
- [6] J. B. Pendry, D. Schurig, and D. R. Smith, *Science* **312**, 1780 (2006).
- [7] U. Leonhardt, *Science* **312**, 1777 (2006).
- [8] U. Leonhardt and T. Philbin, *Geometry and Light: The Science of Invisibility*, Dover Books on Physics (Dover Publications, New York, US, 2010).
- [9] D. Schurig, J. J. Mock, B. J. Justice, S. A. Cummer, J. B. Pendry, A. F. Starr, and D. R. Smith, *Science* **314**, 977 (2006), ISSN 0036-8075.
- [10] J.-P. Berenger, *J. Comp. Phys.* **114**, 185 (1994), ISSN 0021-9991.
- [11] W. C. Chew and W. H. Weedon, *Microwave Opt. Tech. Lett.* **7**, 599 (1994), ISSN 1098-2760.
- [12] Z. S. Sacks, D. M. Kingsland, R. Lee, and J.-F. Lee, *IEEE Trans. Antennas Propag.* **43**, 1460 (1995), ISSN 0018-926X.
- [13] F. L. Teixeira and W. C. Chew, *IEEE Microwave and Guided Wave Letters* **7**, 371 (1997), ISSN 1051-8207.
- [14] R. W. Ziolkowski, *IEEE Trans. Antennas Propag.* **45**, 656 (1997), ISSN 0018-926X.
- [15] F. L. Teixeira, *Radio Sci.* **38**, n/a (2003), ISSN 1944-799X, 8014.
- [16] K. Sainath and F. L. Teixeira, *J. Opt. Soc. Am. B* **32**, 1645 (2015).
- [17] J. B. Keller and W. Streifer, *J. Opt. Soc. Am.* **61**, 40 (1971).
- [18] G. A. Deschamps, *Electronics Letters* **7**, 684 (1971), ISSN 0013-5194.
- [19] L. B. Felsen, *Symposia Mathematica* **18**, 39 (1976).
- [20] E. Heyman and L. B. Felsen, *J. Opt. Soc. Am. A* **18**, 1588 (2001).
- [21] K. Tap, Ph.D. thesis, The Ohio State University, Columbus, Ohio, USA (2007).
- [22] R. F. Harrington, *Time-Harmonic Electromagnetic Fields* (IEE Press, New York, US, 2001).
- [23] J. B. Pendry, *Phys. Rev. Lett.* **85**, 3966 (2000).
- [24] R. E. Collin, *Progress In Electromagnetics Research* **19**, 233 (2010).
- [25] V. G. Veselago, *Soviet Physics Uspekhi* **10**, 509 (1968).
- [26] M. Kuzuoglu, *IEEE Trans. Antennas Propag.* **54**, 3695 (2006), ISSN 0018-926X.
- [27] Note that our definitions of flat-space and deformed (complex-space) coordinates follow much of the PML literature, and are reversed w. r. t. the TO literature. The final material properties are, of course, independent of coordinate convention.
- [28] Note that the integral in Eq. (1) is taking along *decreasing* values of x so that negative σ_x implies $\Im m[x'] > 0$ in Eq. (1) and hence a gain medium.
- [29] These cases resemble, but are not identical, to (isotropic) zero-index and double-negative media respectively, because we are dealing with (doubly) anisotropic media here [26].
- [30] Similar results can be obtained with other mirror-symmetric functions such as, for example, $\sigma_x = \sin(\pi 2x/d)$; however, in this case the transformation media becomes inhomogeneous since the Jacobian is an x -dependent function.